CrossMark

The Impact of Source Distribution on Scalar Transport over Forested Hills

Andrew N. Ross[1] · Ian N. Harman[2]

Abstract Numerical simulations of neutral flow over a two-dimensional, isolated, forested ridge are conducted to study the effects of scalar source distribution on scalar concentrations and fluxes over forested hills. Three different constant-flux sources are considered that span a range of idealized but ecologically important source distributions: a source at the ground, one uniformly distributed through the canopy, and one decaying with depth in the canopy. A fourth source type, where the in-canopy source depends on both the wind speed and the difference in concentration between the canopy and a reference concentration on the leaf, designed to mimic deposition, is also considered. The simulations show that the topographically-induced perturbations to the scalar concentration and fluxes are quantitatively dependent on the source distribution. The net impact is a balance of different processes affecting both advection and turbulent mixing, and can be significant even for moderate topography. Sources that have significant input in the deep canopy or at the ground exhibit a larger magnitude advection and turbulent flux-divergence terms in the canopy. The flows have identical velocity fields and so the differences are entirely due to the different tracer concentration fields resulting from the different source distributions. These in-canopy differences lead to larger spatial variations in above-canopy scalar fluxes for sources near the ground compared to cases where the source is predominantly located near the canopy top. Sensitivity tests show that the most significant impacts are often seen near to or slightly downstream of the flow separation or reattachment points within the canopy flow. The qualitative similarities to previous studies using periodic hills suggest that important processes occurring over isolated and periodic hills are not fundamentally different. The work has important implications for the interpretation of flux measurements over forests, even in relatively gentle terrain and for neutral flow. To understand fully such measurements it is necessary not only to understand the flow structure

✉ Andrew N. Ross
a.n.ross@leeds.ac.uk

[1] Institute for Climate and Atmospheric Science, School of Earth and Environment, University of Leeds, Leeds, UK

[2] CSIRO Oceans and Atmosphere Flagship, Canberra, Australia

(given the site characteristics) but also to know the distribution of scalar sources and sinks in the canopy.

1 Introduction

The issue of advection, or more strictly the divergence of the horizontal fluxes and transport by a mean vertical wind speed, has been an active area of research for some time (e.g., Aubinet et al. 2005; Feigenwinter et al. 2008; Zeri et al. 2010). Attempts to address the issue from an observational perspective have included the use of multiple towers (Feigenwinter et al. 2008), fully enclosed sampling methods (Leuning et al. 2008) and the development of algorithms to identify conditions when the eddy-covariance assumptions are not met (e.g., Goulden et al. 2006; van Gorsel et al. 2007, 2008), with mixed results. While much is known about the symptoms of advection, less is known about the underpinning physical or biophysical origins of the issue. In particular, while detailed analyses have been carried out at a number of sites, there remain key difficulties in taking the understanding gained and applying this to other sites. For example, Belcher et al. (2012) note that the key diagnostic quantities and scales that determine the quantitative impact of the advection terms at any individual site are not really known. This is important as it would allow a more thorough analysis and quantification of the issue, e.g. determining defensible error estimates for the many hundred sites around the world and how this feeds through to the global and regional estimates of, for example, carbon exchange or ecosystem functioning. Such understanding could be used to develop site-diagnostic tools to assist in locating future FLUXNET sites.

A quantitative understanding of how the near-surface flow and turbulence responds to canopies and complex terrain is a necessary precursor to the understanding of how scalars are transported within that flow. This is in itself challenging from an observational perspective (e.g., Zeri et al. 2010; Grant et al. 2015). A range of methodologies have now been developed to quantitatively describe the flow and turbulence, though most concentrate only on neutral conditions. These include simple linearized theoretical approaches developed by Finnigan and Belcher (2004), Belcher et al. (2008), Harman and Finnigan (2013) and colleagues, and numerical simulations of varying degrees of complexity (e.g., Ross and Vosper 2005; Ross 2008; Patton and Katul 2009; Bohrer et al. 2009). Importantly, all of these studies indicate that the presence of a canopy systematically alters the response of the flow to complex terrain, both within and above the canopy, from the more traditional understanding (Hunt et al. 1988; Belcher et al. 1993) even in gentle terrain. These approaches show that the flow and turbulence vary systematically with position in complex terrain, with hill crests particularly prone to significant deviations in the flow vector and intensity of turbulence as compared to the background state with no terrain.

A smaller number of studies have also considered the consequent impact on the transport of scalars through that flow field from a more analytical perspective. Katul et al. (2006) considered the transport of CO_2 emitted by a canopy, with sources dictated by a full ecophysiological model as well as prescribed flux and concentration boundary condition sources, in terrain comprised of simple, repeating sinusoidal ridges. Ross (2011) considered the transport of a general scalar emitted uniformly through a canopy again for sinusoidal ridges. More recently Katul and Poggi (2010) considered the impact of complex terrain on the deposition

of aerosol-sized particles. The issue of inertial particle dispersion over over complex terrain is also of increasing interest due to its importance in the dispersion of seed kernels and vegetation migration, gene flow and pest invasion (Katul and Poggi 2012; Tracktenbrot et al. 2014). In all cases the spatial variability in the flow and transport led to the systematic advection of the scalar within and above the canopy and to spatial variability in the vertical scalar flux that can be measured using the aerodynamic method. For the cases considered the vertical scalar flux at twice canopy height varied by a factor 1.5–2 depending on position in both the Katul and Poggi (2010) and Ross (2011) studies, certainly not insignificant. Katul and Poggi (2011) provided a simple model to explain the aerosol deposition observed in Katul and Poggi (2010). Ross (2011) attempted to place his results in a scaling framework (so that the results can be generalized) although this is a partial analysis that considers the impacts in the upper canopy only.

Scalars are, however, emitted or absorbed in a number of different ways (passed through stomata, respired, deposited) leading to different source distributions and characteristics (prescribed fluxes, prescribed surface concentrations, mixed surface conditions) and a comparison of different scalars with different source characteristics has not been undertaken to date. Raupach et al. (1992) showed that the perturbations to the scalar flux and concentration patterns associated with flow over topography with low roughness are directly controlled by the type of scalar source, so we should expect similar effects when the topography is covered by a canopy. Furthermore the consideration solely of terrain with simple sinusoidal ridges ignores the fact that more realistic terrain could produce different impacts (usually smaller) with different spatial patterns (e.g., Harman and Finnigan 2010). Here we seek to address two questions: firstly what role does source distribution play in governing the transport of scalars within and above canopies in complex terrain? Secondly, does the sinusoidal periodicity in the terrain considered to date affect our ability to draw general conclusions from more isolated hills?

2 Methodology

The conservation of a scalar tracer c in turbulent flow can be written as

$$\frac{\partial C}{\partial t} + U_j \frac{\partial C}{\partial x_j} = -\frac{\partial \overline{u'_j c'}}{\partial x_j} + S, \tag{1}$$

where c is the molar concentration, u_j is the wind vector and S is the source/sink of the scalar (zero above the canopy). Here the overline indicates both a temporal and local spatial average with upper case letters indicating the averaged quantity and primes the instantaneous and local deviations from the average. (A more rigorous discussion of the averaging procedure in canopies can be found in e.g. Finnigan 2000). Molecular diffusion is neglected and the summation convention assumed; S represents release/uptake of the scalar by the canopy. Equation 1 requires boundary conditions for solution, which permits further sources/sink terms at the boundaries e.g. to represent release/uptake of the scalar by the soil. Alternatively concentration boundary conditions could be applied, although they are not considered further here.

In steady-state conditions, invoking continuity of the mean flow and applying a first-order closure for the turbulent fluxes with isotropic diffusivity, K_c, Eq. 1 simplifies to

$$\frac{\partial C}{\partial t} = -\frac{\partial U_j C}{\partial x_j} + \frac{\partial}{\partial x_j}\left(K_c \frac{\partial C}{\partial x_j}\right) + S = 0. \tag{2}$$

Given forms for the mean wind field, U_j, the turbulent scalar diffusivity, K_c, and the source/sink, S, Eq. 2 can be solved numerically to provide an estimate of the scalar concentration field.

The ratio of the turbulent momentum diffusivity, K_m to the turbulent scalar diffusivity defines the Schmidt number $S_c = K_m/K_c$. For neutral flow, observations suggest a value of ≈ 1 in the atmospheric boundary layer above the canopy, with values of ≈ 0.5 at canopy top (Raupach et al. 1996). Huang et al. (2013) showed a connection between coherent canopy-flow structures and the turbulent Schmidt number in their large-eddy simulation study. Large-eddy simulations over flat ground by Ross (2008) showed reduced Schmidt numbers just above the canopy, but enhanced Schmidt numbers (up to about 1.5) deeper within the canopy. The presence of a small hill led to variations in the Schmidt number across the hill, with larger values than occurred over flat ground at most locations and heights within and just above the canopy. With a mixing-length closure scheme the Schmidt number has to be specified. For simplicity, and in the absence of more detailed information on what the correct Schmidt number should be in canopies over complex terrain, we take $S_c = 1.0$ everywhere in this study.

Numerical solutions to this problem were found using the BLASIUS model, which has been used for a number of previous canopy-flow studies (e.g. Ross and Vosper 2005; Ross 2011). The model solves the time dependent Boussinesq equations in a terrain-following coordinate system, and a 1.5-order turbulence closure scheme is used. The flow is driven by an imposed pressure gradient, balanced by a constant geostrophic wind (here taken as $10\,\mathrm{m\,s}^{-1}$) at the top of the model domain. The canopy is parametrized through a drag term, $-c_d a \mathbf{u}|\mathbf{u}|$ in the momentum equation (where c_d is a local drag coefficient and a is the leaf area density), a constant mixing length in the canopy and an enhanced dissipation rate due to the rapid conversion of energy from the large to small scales by the work against canopy drag. Details of the scheme are given in Ross and Vosper (2005). The canopy is parametrized in terms of the canopy drag coefficient ($c_d = 0.25$), the canopy leaf area density ($a = 0.4\,\mathrm{m}^{-1}$), the canopy height $h_c = 10\,\mathrm{m}$ and displacement height $d = 8.65\,\mathrm{m}$. The canopy leaf area density and canopy drag coefficient are assumed constant with height in the canopy. While this is not completely realistic, Finnigan and Belcher (2004) showed that this is a sufficient condition for first-order mixing-length closure schemes to be a good approximation to a full second-order closure, at least for the turbulent transport of momentum. Other relevant canopy parameters are derived using the relationship given in Ross and Vosper (2005), so $l = \kappa(h_c - d) = 0.54\,\mathrm{m}$ where κ is von Karman's constant, the canopy adjustment length scale, $L_c = 1/(c_d a) = 10\,\mathrm{m}$, and the momentum absorption efficiency $\beta \equiv u_\star/U_h = (l/(2L_c))^{1/3} = 0.3$, with $u_\star$ the friction velocity and U_h the wind speed at canopy top when the canopy is on level ground. These canopy parameters are taken as fixed in all simulations presented here unless otherwise stated.

The model is run first as a one-dimensional (1-D) model to obtain a steady-state background profile (100000 s), and the results used to initialize a 2-D simulation, which is again run to steady state (1000 s). Initializing the 2-D simulation with the 1-D profile speeds up convergence in the 2-D simulation considerably. Periodic lateral boundary conditions are imposed, with a no-slip boundary condition at the floor of the canopy. The aerodynamic roughness length, $z_0 = 0.35\,\mathrm{m}$, is relatively high, but consistent with Ross and Vosper (2005). A domain depth of 1500 m is used, with a domain width of 2000 m, while there are 80 grid points in the vertical with a stretched grid. The vertical resolution near the ground is 0.5 m with a stretch factor of 1.05, giving 12 grid points within the canopy for $h_c = 10\,\mathrm{m}$. At the upper boundary the geostrophic wind speed is prescribed.

In this study we consider the response of the scalar concentration field in idealized complex terrain, a single isolated two-dimensional ridge oriented normal to the geostrophic flow. The isolated ridge surface considered is given analytically by

$$z_{hill} = H \exp\left\{-x^2/L^2\right\}, \tag{3}$$

with $H = 10$ m and $L = 200$ m. This hill satisfies the small-slope conditions of Finnigan and Belcher (2004) for their analytical model to be valid (the maximum slope for these values of L and H is approximately 2.5°) though not the restriction on canopy depth. The scaling arguments outlined in Ross (2011) indicate that, for this hill-canopy combination, the scalar mean advection terms are small compared to the source strength. The horizontal domain is 2000 m $= 10L$ and so the ridge can be considered isolated; there are 128 grid points in the horizontal and so the ridge is well resolved. In what follows z is the vertical height above the surface and x is the horizontal position. The velocity components u and w are the true horizontal and vertical velocities respectively.

The primary focus here is the differing response of the scalar concentration profiles with position across complex terrain, as governed by different source/sink profiles. All simulations are therefore performed with the same canopy, hill and dynamical fields, but with various source / sink configurations. In reality the sources and sinks of the important scalar species are driven by a complex mix of physical and biological processes, including photosynthesis, heterotrophic and autotrophic respiration and the surface energy balance. To reduce this complexity we consider four stylized forms for the scalar source distribution. Three of the sources are prescriptions of the flux and given analytically by

$$S(x, z) = \begin{cases} S_0/h_c & \text{if } z \leq h_c \quad \text{uniform source,} & \text{(4a)} \\ S_0\alpha(z - h_c) \exp(z - h_c)/L_R & \text{if } z \leq h_c \quad \text{radiation source,} & \text{(4b)} \end{cases}$$
$$\overline{w'c'}(z = 0) = S_G \qquad\qquad\qquad\qquad \text{ground source.} \tag{4c}$$

These three forms for the source are canonical representations for conditions when the scalar source is uniformly distributed through the canopy (as in Ross 2011), when the scalar source is controlled by a depth-varying process similar to photosynthesis, and when the scalar source is located at the ground. For ground sources the scalar roughness length associated with the boundary layer is $z_{0c} = 0.05$ m. In Eq. 4 S_0 and S_G control the total source magnitude (given in mol m^{-2} s^{-1}), L_R is a depth scale controlling the variation of the source distribution within the canopy, and $\alpha(L_R)$ is a parameter used to scale the source strength to ensure the depth-integrated source equals S_0. These three source profiles are particularly useful as their distribution bridges the case where the source is predominately emitted in the upper canopy ('radiation source' with L_R small) to the case where the scalar is entirely emitted at the ground. The respective impacts on the scalar concentration with position then provide insight into the relative importance of the different processes involved in the flow transport of scalars in complex terrain.

The fourth scalar source considered is a prescription of the canopy-element surface scalar concentration (the rUC source). The rUC source is then given by (Harman and Finnigan 2008)

$$S(x, z) = \frac{c_d a}{2} r|\mathbf{U}|(C(x, z) - C_0) \tag{5}$$

if $z \leq h_c$, where C_0 is the element surface value of the scalar concentration and $r \approx 0.1$ is a leaf-level Stanton number. Unlike the prescribed sources in Eq. 4 the rUC source strength can vary with position (and even change sign) (see also Katul et al. 2006).

For all source types an equal and opposite sink term is distributed over a layer at the top of the domain in order to ensure the total scalar is conserved and hence a steady state is possible. There is zero scalar flux at the top of the domain.

In the next section we show how the scalar concentration varies with position across the specified isolated ridge and with source distribution.

3 Results

3.1 Impact of Scalar Source Distribution

The importance of the source type and distribution is illustrated by simulating the concentration fields and associated transport terms within the flow over a single isolated, gentle ridge covered by a uniform canopy with the different sources described above. The canopy and flow parameters are fixed, as described above. For the three source terms with a prescribed flux we take $S_0 = S_G = 1 \, \text{mol m}^2 \, \text{s}^{-1}$ with $L_R = 1 \, \text{m}$ for the radiation source. For the rUC source we take $r = 0.1$ and $C_0 = 100 \, \text{mol m}^{-3}$. Figure 1 shows the background, flat terrain, profiles of the source strength, the difference in scalar concentration from a reference value at height $z = 5h_c$, and the vertical turbulent scalar flux as obtained with the mixing-length closure. The normalization scales are the friction velocity u_* and turbulent scalar scale c_* as calculated from the constant-flux layer just above the canopy. Despite the normalization, and that three of the four cases have an identical depth-integrated source strength, there is a difference in depth-integrated scalar concentration. This is because the use of the first-order closure requires vertical gradients in the concentration sufficient to support the (prescribed) flux. Consequently, the cases where the source is located in the upper canopy ('radiation' and 'rUC' cases) lead to smaller gradients and differences in scalar concentration through the canopy. For the case of the ground source, the turbulent diffusivity is so small near the ground that significant gradients are required to support the flux. Given that advection becomes a problem for eddy covariance in the presence of gradients (in the wind field and/or concentration fields) then this suggests a priori that estimates of the strength of ground-based sources are more likely to be affected by advection than are upper canopy sources.

Figure 2 shows the results of the model for the streamwise component of the wind vector (a), the vertical velocity (b), and the turbulent diffusivity K_c (c) with position over the ridge. Note that, despite being of gentle slope, the canopy height ($h_c = 10 \, \text{m}$) and canopy density scale ($L_c = 10 \, \text{m}$) are sufficient to generate regions of reversed flow within the canopy, which are driven by the balance between shear stress, aerodynamic drag and the hill-induced pressure perturbation (Finnigan and Belcher 2004), including well upstream from the ridge. The changes in the turbulent diffusivity across the ridge appear small, except in the deep canopy. However, as noted earlier, even small changes in the diffusivity can lead to large changes in the scalar concentration profile and concentration gradients so these cannot be deemed inconsequential without further study. The diffusivity changes are mainly located near to the ground and originate from changes to the near-ground wind speed and the associated boundary layer.

Figures 3 and 4 show the steady-state fields of the normalized scalar concentration difference and vertical scalar fluxes across the isolated ridge. Qualitatively the pattern of the impact is similar across the four cases and also similar to the results shown in Katul et al. (2006) and Ross (2011). In particular the largest impacts are seen around the convergence/divergence zones in the simulated wind field (i.e. at hill crest and near the bottom of the ridge, see Figs. 2
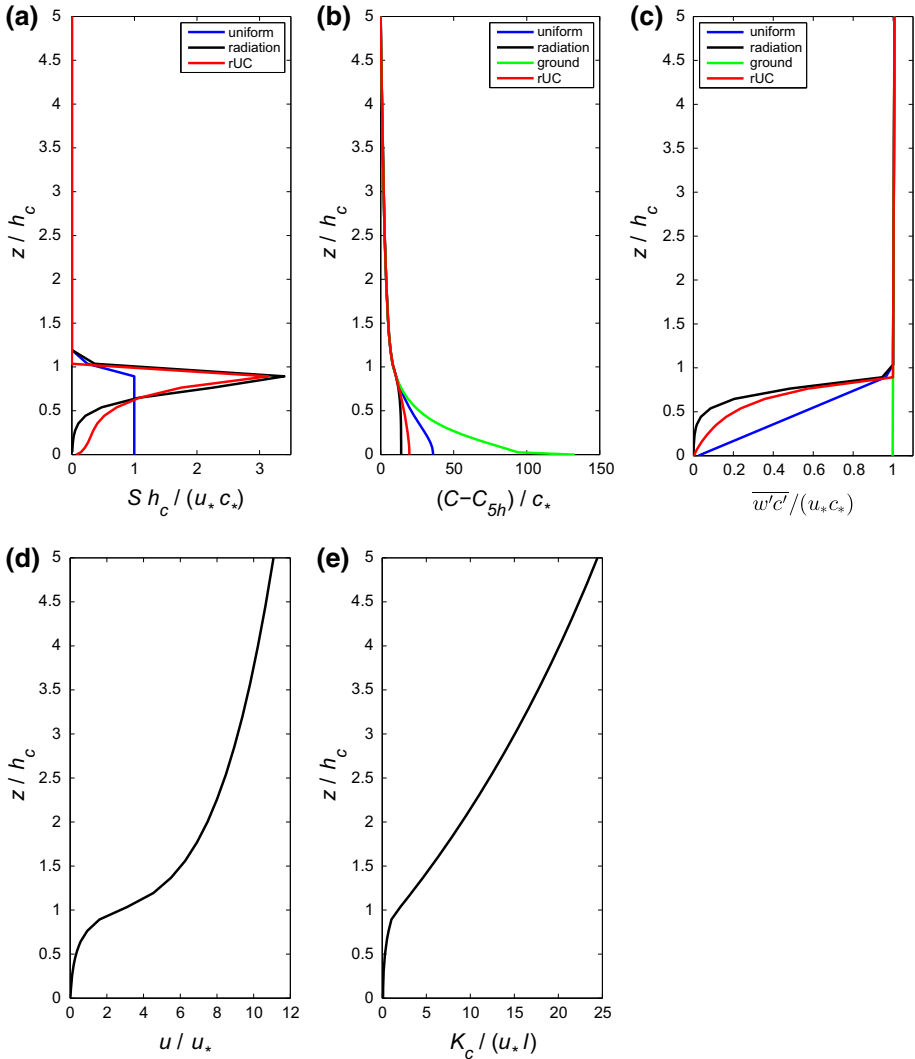
Fig. 1 Normalized background profiles of **a** scalar source term, **b** scalar concentration, **c** turbulent scalar flux in the absence of a hill, **d** horizontal velocity and **e** turbulent diffusivity. The *lines* in **a**–**c** are for the different sources: uniform (*blue*), radiation (*black*), ground (*green*) and rUC (*red*)

and 3). These are the regions with the largest vertical motion in the canopy that enables a systematic transport of air with different scalar concentration into/out of the canopy, and/or low values of the turbulent diffusivity within the canopy, which enables the establishment of large scalar concentrations for transport by the mean flow. From the streamlines it is clear that the vertical motion near canopy top is relatively weak for this hill, although it is more important deeper in the canopy in the proximity of the regions of separated flow. Nonetheless it does have a marked effect in modulating scalar concentrations across the hill.

Figure 5 shows the normalized vertical scalar flux at twice canopy height (left) and three times canopy height (right) above the ground with position across the hill for the four source
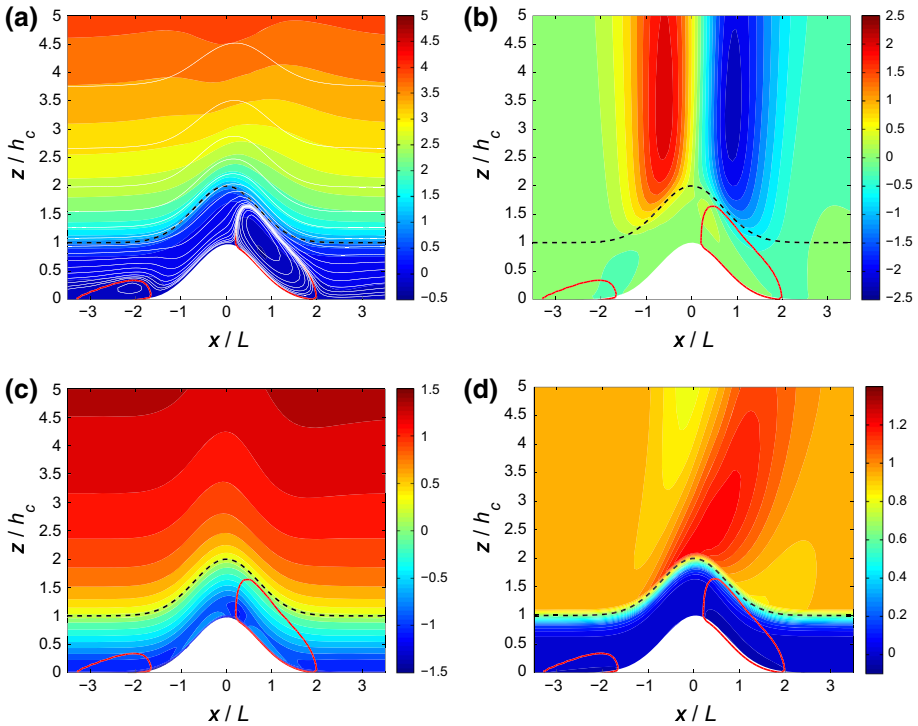
Fig. 2 Contour plots of the **a** normalized horizontal velocity, U/U_h, **b** normalized vertical velocity, $W/(U_h H/L)$, **c** normalized eddy viscosity, $K_c/(u_\star l)$ on a $\log_{10}$ scale and **d** the normalized vertical momentum flux, $\overline{u'w'}/(-u_\star^2)$. The *black dotted line* marks the canopy top and the *solid red line* is the dividing streamline delineating regions of flow separation. The *thin white lines* on **a** show other streamlines of the flow, logarithmically spaced. Not all of the numerical domain is shown

distributions. This shows that, depending on (a) the tower location, and (b) the source type and distribution, location-specific observations of the vertical scalar flux can be significantly biased with respect to the actual source strength. The spatial pattern is non-symmetric around the value of 1 as a result of the background concentration profile and the lack of vertical symmetry that leads to the regions of positive and negative vertical velocity being of different sizes. This asymmetry indicates that local measurements of the vertical scalar flux somewhat underestimate the true source strength as a consequence of the flow and transport except within small regions where the observations provide a large overestimate. This implies a general tendency to underestimate the scalar eddy-covariance flux from towers randomly positioning in the landscape. Furthermore the local measurements of scalars with ground-based sources are clearly more affected than those with sources in the (upper) canopy. The different impacts on scalars with different sources also suggest that knowledge about the likelihood of impacts on one scalar cannot necessarily be used to infer impacts on other scalars with different source/sink distributions (e.g. energy balance closure and CO_2 closure).

The scalar concentration and flux fields from different source distributions can be superimposed if they are all prescribed by flux boundary conditions. Figure 5 also shows horizontal profiles of the vertical turbulent flux across the ridge for two cases with more realistic combined sources, (i) 'Balanced' with a ground source exactly balanced by a canopy sink (i.e.
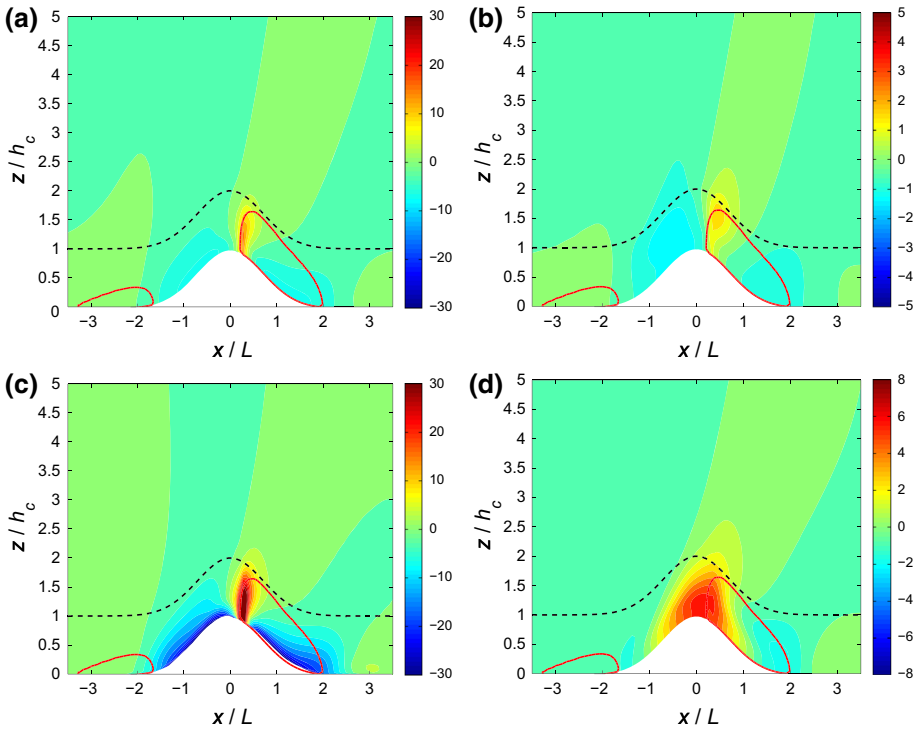
Fig. 3 Contour plots of scalar concentration perturbation fields (2-D minus 1-D field), normalized by $c_\star$, for different source types: **a** uniform source, **b** radiation source, **c** ground source and (**d**) rUC source. The 1-D field is the steady state solution over flat terrain shown in Fig. 1. The *black dotted line* marks the canopy top and the *solid red line* is the dividing streamline delineating regions of flow separation. Note the different colour scales on the different subfigures

surface respiration balancing net canopy assimilation) and hence the net source strength is zero; (ii) 'Midday' with a canopy sink strength that is three times that of a ground source (i.e. typical of a midday balance of carbon sources/sinks) and hence the net source strength is $-S_0$. For case (i) where there is no net source of scalar, a non-zero local vertical flux is nevertheless observed across the ridge. Near the region of flow separation this is significant (up to $0.9S_0$), with a smaller magnitude negative flux balancing elsewhere over the slopes. This feature arises because of the relatively larger impact on the scalar concentrations and flux patterns for the ground source as compared to the radiation source. For case (ii) with the same net source as before, the fact that the concentration associated with the ground source shows a much larger response to the ridge means that it dominates the spatial patterns, even though it is smaller by a factor of three than the radiation source term. The net effect depends on sensor height and does not follow the pattern followed by either single source term. As the balance between the different source changes, e.g. through the day or with the season, the topographically-induced bias in local fluxes can therefore vary significantly.

3.2 Budget Analysis

To fully understand the origins of these results, especially with regard to their robustness to modelling specifics, it is useful to separate out the different terms in the scalar equation (Eq. 2).
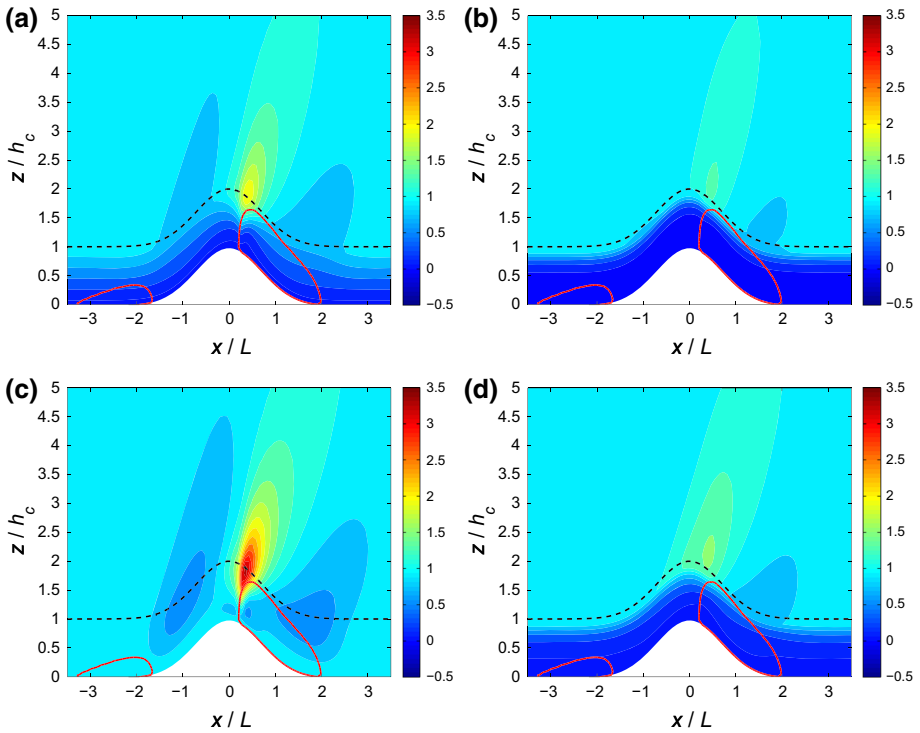
Fig. 4 Contour plots of vertical scalar turbulent flux normalized by $u_\star c_\star$, for different source types: **a** uniform source, **b** radiation source, **c** ground source and **d** rUC source. The *black dotted line* marks the canopy top and the *solid red line* is the dividing streamline delineating regions of flow separation
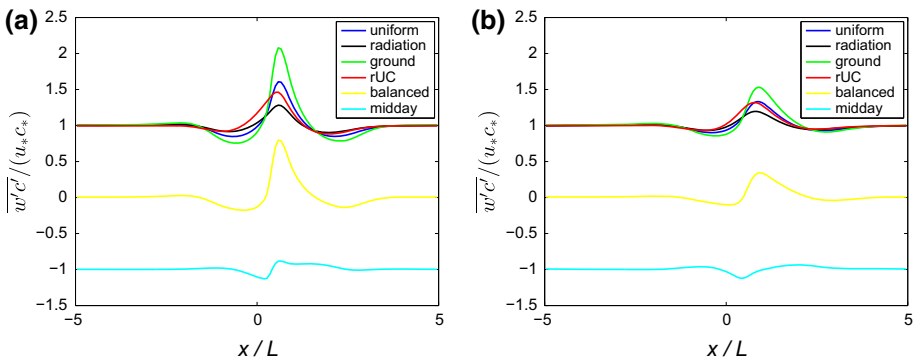

Fig. 5 Profiles of turbulent scalar flux normal to the mean flow at **a** height h_c and **b** height $2h_c$ above the canopy top for the different source types. In addition to the four standard source types, lines are also included for two combined sources. The first ('balanced') has equal and opposite ground source and radiation sink terms of strength S_0, and therefore the net source term is zero. The second ('midday') mimics daytime photosynthesis and soil respiration and has a radiation sink of strength $-1.5S_0$, and a ground source term of strength $0.5S_0$. The net source is therefore equal to $-S_0$
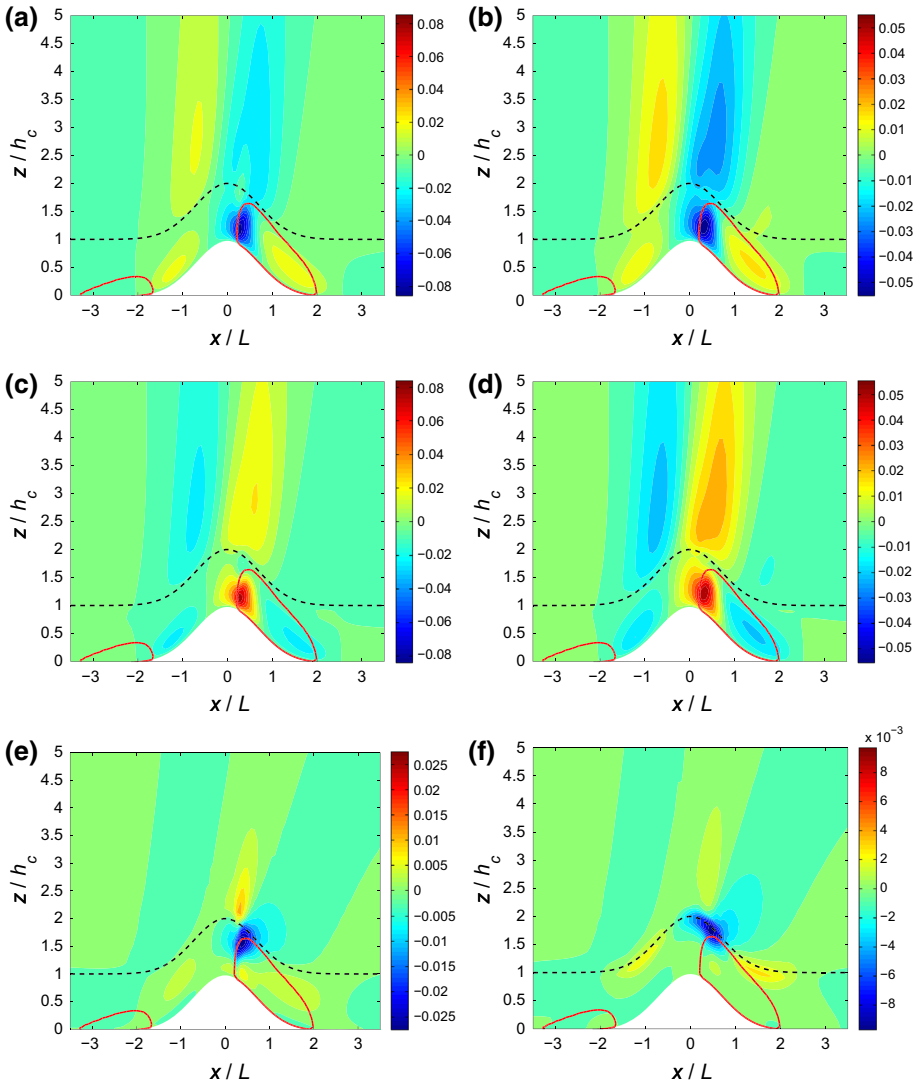
Fig. 6 Contour plots of horizontal scalar advection (**a**, **b**), vertical scalar advection (**c**, **d**) and total scalar advection (**e**, **f**) terms for the uniform source (**a**, **c**, **e**) and the radiation source (**b**, **d**, **f**). The *black dotted line* marks the canopy top and the *solid red line* is the dividing streamline delineating regions of flow separation. Note the different *colour* scales in each plot

Figure 6 shows the horizontal and vertical components of the advection term ($\partial UC/\partial x$ and $\partial WC/\partial z$ respectively) as well as the total advection term ($\partial UC/\partial x + \partial WC/\partial z$) for the uniform source and the radiation source, while Fig. 7 shows the horizontal and vertical components of the turbulent-flux divergence ($\partial \overline{u'c'}/\partial x$ and $\partial \overline{w'c'}/\partial z$). For large regions of the ridge and surroundings the divergence of both the turbulent flux and the mean advection terms are small. These small values however are necessary to establish the spatial patterns in the scalar concentration and scalar turbulent flux.
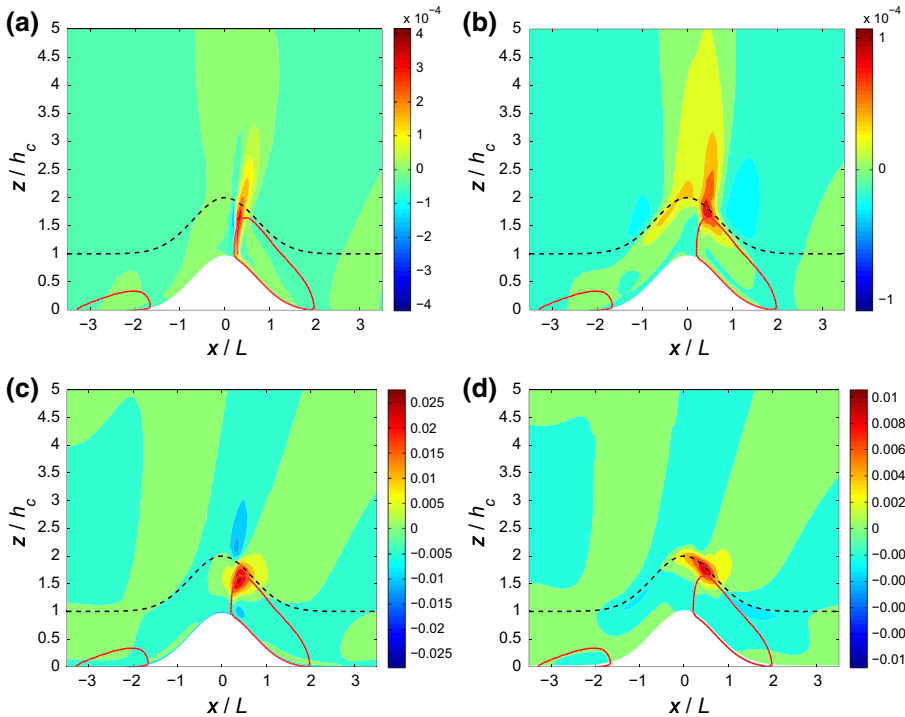
Fig. 7 Contour plots of perturbations in the horizontal (**a**, **b**) and vertical (**c**, **d**) turbulent scalar flux divergence terms for the uniform source (**a**, **c**) and the radiation source (**b**, **d**). The *black dotted line* marks the canopy top and the *solid red line* is the dividing streamline delineating regions of flow separation. Note the different *colour* scales in each plot

The individual advection terms in Fig. 6 are larger in magnitude, however the horizontal and vertical components largely cancel out over most of the flow field (see e.g. Finnigan 1999). If the advection terms are not written in flux form (as in Eq. 1) then the individual terms are even larger (not shown). The net effect of advection is therefore a balance of two large, but largely cancelling, terms. To observe the advection terms in the field it is therefore necessary to carefully measure both horizontal and vertical advection terms and to do so to a high level of accuracy to ensure the net sum is accurately calculated.

In contrast, around the regions of convergence in the U field, both advection and turbulent-flux divergence are large. In the region of the separation point near the hill crest these patterns arise from the streamwise convergence of the mean flow and scalar enriched air within the canopy ($\partial UC/\partial x < 0$), with corresponding transport by the mean flow vertically (and a mean flux divergence $\partial WC/\partial z > 0$). Following the mean flow, the scalar enriched air is transported upwards into the upper canopy where it is rapidly mixed due to increased turbulence. Consequently, the vertical turbulent flux is increased markedly and associated gradients in all four transport terms occur (and in particular $\partial WC/\partial z < 0$ and $\partial \overline{w'c'}/\partial z > 0$). Similar, but countersigned, arguments lead to the patterns at the base of the ridge in Figs. 6 and 7, with the reduced magnitude due to the natural vertical asymmetry in the background scalar concentration and proximity to the ground. Qualitatively the results in Fig. 6 are similar to those presented in Katul et al. (2006) despite the analytical flow field, but more complicated ecophysical source model, used in that study.

While both the uniform and radiation sources lead to broadly similar patterns in the advection and turbulent-flux divergence, there are some important quantitative differences between the two cases, despite both having identical velocity fields. The most noticeable feature is that the magnitudes of the advection and turbulent-flux divergence terms are smaller with the radiation source. There are also differences in the location of the maximum in the advection terms. The differences are due to the different scalar concentration fields resulting from the different source distributions. With the radiation source located in the upper canopy the scalar concentrations and vertical scalar gradients are smaller in the deep canopy than in the constant source case, and so advection plays a lesser role here. Instead, with the radiation source, the advection term is most important in the upper canopy where the largest scalar gradients occur. The individual, and largely cancelling, horizontal and vertical components of the advection terms look quite similar between the two cases, but the sum of the terms shows distinctive patterns near canopy top, again highlighting the difficulties in measuring the effect of advection in the field. A similar pattern to the net advection is seen in the vertical turbulent flux divergence term.

Turbulent transport is dominated by the vertical term. The horizontal turbulent-flux divergence term is largest near the leading edge of the separation bubble, and even there it is two orders of magnitude smaller than the vertical turbulent-flux divergence. This is in line with scaling arguments and previous work (Finnigan 1999) and suggests that from an observational point of view it is not necessary to measure these terms, at least for a passive scalar.

Both the advection and perturbations to the turbulent divergence terms are only (really) large in the convergence/divergence zones within the canopy. This implies that these could be, (a) sensitive to the numerical schemes used, (b) sensitive to resolution, and (c) sensitive to the turbulence parametrization. We expect flow separation to be a ubiquitous feature of canopy flows over hills. The analytical model of Finnigan and Belcher (2004) shows this to be driven by the adverse pressure gradient over the lee slope that is, to leading order, an inviscid process and therefore insensitive to the details of the turbulence scheme. The qualitative physical reasoning is therefore robust and so we would expect to see a similar balance of terms to that shown here, although the precise details may be dependent on the model specifics.

3.3 Sensitivity to Model Parameters

There are a number of non-dimensional parameters (h_c/L_c, L_c/L, H/L, h_c/H) controlling the flow and scalar transport over idealized forested ridges such as these. The sensitivity of the results to the three independent parameters (L_c/L, h_c/L_c and H/L) is investigated through a series of simulations. The canopy density remains fixed throughout so L_c is unchanged. To vary L_c/L both L and H are changed keeping h_c/L_c and H/L fixed, and to vary h_c/L_c the canopy height h_c is changed with the hill remaining fixed. Changes in H/L are made by changing H. In all these simulations the unchanged parameters take the same values as given in Sect. 2. For simulations where L were varied, the width of the domain and the number of horizontal grid points were scaled with L to ensure that the horizontal resolution remained constant. In each case the magnitude and location of the maximum and minimum of the scalar-flux term at height h_c above the canopy is plotted as a function of the varying non-dimensional parameter (L/L_c, h_c/L_c and H/L) (see Fig. 8).

The maximum and minimum changes in the above-canopy scalar flux increase with increasing L_c/L, h_c/L_c and H/L. In each case increasing the non-dimensional parameter leads to an increase in the induced flow perturbation, and hence an increase in the scalar-flux perturbations. The dynamical changes are, at least qualitatively, entirely consistent with the
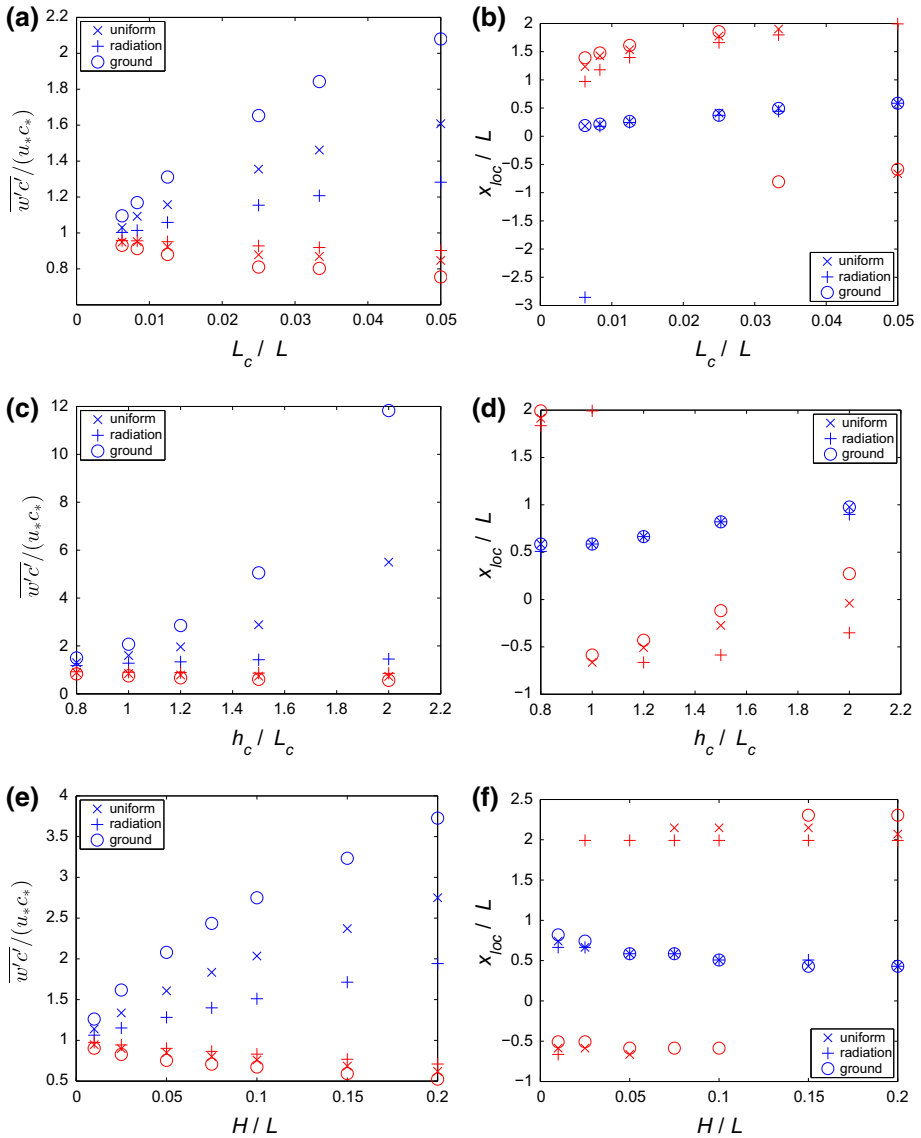
Fig. 8 Plots of the magnitude (**a, c, e**) and location, x_{loc}, (**b, d, f**) of the maximum (*blue*) and minimum (*red*) turbulent scalar flux normal to the mean flow at a height of h_c above the canopy as a function of L_c/L (**a, b**), h_c/L_c (**c, d**) and H/L (**e, f**). The different source distributions are marked with different *symbols*

dependence of the perturbed flow on L_c/L, h_c/L_c and H/L seen in the analytical solution of Finnigan and Belcher (2004) and in the numerical simulations of Ross and Vosper (2005) over infinite periodic hills. Variations in the location of the flow separation and reattachment points, which are key to understanding the changes to the scalar fluxes, are due to second-order terms as discussed in Ross and Vosper (2005) and Harman and Finnigan (2013). The pattern of ground sources having more impact than radiation sources on the above-canopy flux perturbations for a given canopy and hill is a consistent feature across all these sim-

ulations. The location of the maximum canopy flux is strongly tied to regions of the flow where $\partial U / \partial x < 0$, for example the flow separation point just downwind of the hill summit. In these sensitivity tests the only case for which the maximum is not located at the flow separation point is for the radiation source and the smallest value of L_c/L. In this case the perturbed flow and the changes in the scalar flux are negligible anyway. The flux minimum is often located near the re-attachment point of the flow over the lee slope. There is also a local above-canopy flux minimum over the upwind slope where penetration of the mean flow into the canopy reduces the scalar concentration gradient and the turbulent flux above the canopy. Both of these are associated with $\partial U / \partial x > 0$. For some non-dimensional parameter values the minimum on the upwind slope can be the global minimum in the above-canopy scalar flux. Which of the two local minima is more significant appears to vary smoothly with the non-dimensional parameters. Small L_c/L, small h_c/L_c and large H/L tend to lead to the minimum near the re-attachment point being most significant, while the upwind minimum dominates for large L_c/L, large h_c/L and small H/L values. The precise transition point between these two behaviours depends not just on the dynamics, but also on the source distribution, with the ground sources tending to undergo transition earlier to an upwind flux minimum becoming dominant.

Overall this sensitivity analysis shows that, as might be expected, the magnitude of the effects increases as the flow perturbations induced by the hill increase (narrow hills, deeper canopies, steeper slopes). The flow separation point is almost always important, particularly for controlling where the maximum observed fluxes are located. Minimum values can be due to either flow into the canopy near the re-attachment point, or alternatively due to the mean flow into the canopy over the upwind slope, particularly when the induced flow is larger. In these idealized simulations these appear to be robust features of the flow over a range of canopy and hill parameters and also different source terms. Of course, in reality we know that flow separation and re-attachment is unsteady and sensitive to other processes such as stratification and canopy density in the trunk space (see e.g., Belcher et al. 2008; Patton and Katul 2009; Poggi and Katul 2007) and so these results cannot be directly used to assess if a particular time period of scalar-flux measurement is affected by these processes. The present results do however provide a qualitative indication of the likely effects of complex terrain on above-canopy scalar fluxes over a range of conditions.

4 Discussion

From the results presented here it is clear that the location of sources or sinks in a forest canopy over complex terrain has a significant impact on the above canopy variability in scalar concentrations and fluxes. Sources that are at the surface (ground source), or inject a significant amount of the scalar into the deep canopy (uniform source), lead to greater variability compared to those sources where the scalar is predominantly injected in the upper canopy (radiation and rUC sources).

To understand this we first consider the case over flat ground where the steady-state scalar profile can be understood as a simple balance between the source term and the scalar turbulent flux divergence in the canopy (advection plays no role in a steady 1-D solution). Sources with significant input of scalar into the deep canopy require there to be a flux divergence into the deep canopy (assuming a flux-gradient relationship holds). This requires a large vertical gradient in the scalar concentration field since the turbulent diffusivity is low in the deep canopy.
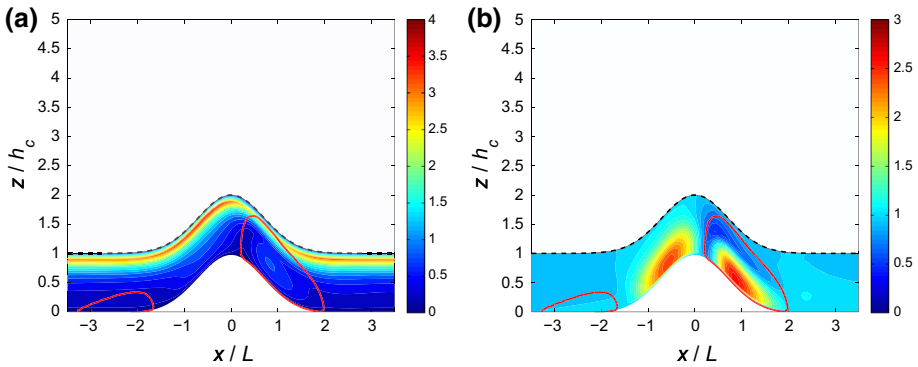
Fig. 9 Contour plots of **a** tracer source term, $S(x, z)$, for the rUC source and **b** normalized source term, $S(x, z)/S_{1d}(z)$, for the rUC source, where $S_{1d}(z)$ is the source term for a flat, homogeneous canopy

For the 2-D case, the steady-state scalar solution is a subtle balance between the source, the turbulent scalar-flux divergence and the scalar advection terms. The presence of a hill induces non-linear flow perturbations in the deep canopy that are large compared to the background flow, and so variations in the eddy diffusivity and advection are much more important for sources near the ground. Hence these sources display the largest variations in scalar concentration and turbulent fluxes.

The variations in scalar concentration and wind speed across the hill can have some impact on the total source from the canopy with sources that depend on the atmospheric scalar concentration. For example, with the 'rUC' source there is a 2.3 % increase in the average scalar source compared to that from a canopy over flat ground. This is small, but not negligible, and is due both to changes in U and C. Locally, changes in the source term are larger, as shown in Fig. 9. In absolute terms the 'rUC' source is largest near the top of the canopy and decays with depth as U decreases. In relative terms, however, the biggest effect is seen deeper in the canopy over the ridge slopes. Over both the upwind and lee slopes there is a marked increase in the source term by up to a factor of three due to the induced flow in the canopy over the hill. In contrast, there is a decrease in the source in the upper canopy over the lee slope, again driven primarily by the reduction in wind speed in the upper canopy (see Fig. 2a). Obviously this is a simple idealization of the actual response of photosynthesis to changes in CO_2 concentration in a canopy but, consistent with Katul et al. (2006), it suggests that the dynamics of canopy flow over complex topography can have a direct influence on the total CO_2 uptake by the forest, aside from any physiological changes due to other ambient changes in climate (e.g. temperature or wind speed with height).

The differences in fluxes persist to several canopy heights, and so there are important implications of these results for interpreting flux measurements from single towers and scaling them to estimate total forest sources and sinks of CO_2 and other scalars (as noted by Ross 2011). Estimating net ecosystem exchange (NEE) at flux-tower sites also requires an estimate of the changes in CO_2 storage within the canopy, often achieved using a profile of high resolution concentration measurements. The advection terms may also affect such estimates of NEE through two additional processes. In steady flow, changes in the storage at a particular location may not be representative of the whole canopy because of the inhomogeneity of the scalar field. Furthermore, changes in storage may often be accompanied by changes in the mean flow and turbulence, which will probably result in changes to the scalar concentration patterns and scalar advection. Such changes will depend on the site, the canopy and on the

meteorological conditions and so will likely need to be considered on a case-by-case basis. All this is for neutral flow and for very small hills, and is therefore separate to the well-documented issues related to drainage flows and nocturnal flux measurements. Ross (2011) gave a scaling analysis to estimate the impact of this effect for a uniform scalar source and for given canopy parameters. Here we show that knowing the details of the canopy is not sufficient. Different source distributions produce different responses above the canopy (see Fig. 5), even for the same total source strength, and so in order to interpret flux measurements from above the canopy one must know something about the source distribution in addition to the canopy structure. This is a challenging requirement.

In contrast to previous studies (e.g., Ross 2011), our study uses an isolated ridge rather than periodic terrain. While this makes some quantitative difference to the results, the qualitative picture is unchanged, with the largest perturbations to the scalar concentration being observed near the stagnation point, just downstream of the summit, and the largest scalar fluxes being observed above the upper part of the lee slope. Further down the lee slope, and over the upwind slope, fluxes above the canopy are actually slightly reduced. The effect of the hill on the fluxes can be observed up to $3L$ upwind of the summit and $3.5L$ downwind of the summit at a height of $2h_c$. At a height of $3h_c$, the impact on the fluxes is smaller, but the effects are seen even further downwind, up to $4L$ from the summit. At a distance of $4L$ the ridge has reduced to 1/16 of its peak height. To avoid the effects of the ridge on flux measurements instruments should be located away from the summit.

One potential limitation of this work is the assumption that we can use a simple mixing-length turbulence closure for the turbulent transport of momentum and scalars within the canopy. There are acknowledged failings of mixing-length closures in strongly distorted flows, or in canopies with rapid changes in foliage distribution (see e.g Finnigan et al. 2015, in press). Finnigan and Belcher (2004) showed theoretically that, for turbulent transport of momentum, the closure assumptions are reasonable for a uniform canopy density. Momentum fluxes are most significant in the upper canopy where the closure assumptions hold well. There is more uncertainty in the lower canopy, however typically velocities and velocity gradients are small there and so momentum transport is not significant anyway. The situation is slightly more complicated for scalar transport, since there may be significant scalar concentration gradients lower down in the canopy, particularly for ground sources. This introduces a quantitative uncertainty into these results, however the key physical processes controlling the variations in scalar concentration and fluxes, namely flow deceleration and flow separation, are essentially inviscid processes driven by the hill-induced pressure gradient (Finnigan and Belcher 2004). One would therefore expect to see qualitatively similar results with different turbulence closure schemes.

We finally reiterate that these simulations consider topography that would not usually be considered complex by the eddy-covariance community and are for neutrally stratified flow. These results are primarily the consequence of the additional physical processes that occur when the canopy flow interacts with topography. Isolated two-dimensional topography results in a larger magnitude of the hydrodynamic pressure perturbation than for isolated three-dimensional topography for the same hill characteristics (e.g., Hunt et al. 1988). Boundary-layer flow is inevitably somewhat unsteady in wind direction and speed that tends to smooth out topographically-locked flow features (e.g., Patton and Katul 2009). Hence it is to be expected that these simulations overstate the topographic impacts on the transport of scalars at real sites. Nevertheless, the magnitude of the simulated impact is not trivial nor would these impacts necessarily be obvious without additional observational constraints.

There are then clear pressing knowledge gaps for the eddy-covariance community that are raised by this study. The first is an ability to routinely assess whether a particular site is

potentially affected by advection and to place error bounds on the possible impacts. Scale analysis (Ross 2011) while helpful will not necessarily identify suitable sites, given the fine balance of physical processes occurring (there are at least five independent length scales to the problem). This is separate from, but related to, requirements around instrumentation footprints in complex terrain (e.g., Finnigan 2004). Second, and far more challenging, is an ability to correct existing data for the impacts of topographic/complex terrain effects. The assimilation of eddy-covariance data into a simple flow-transport model provides one potential method for achieving this aim.

5 Conclusions

Returning to our initial questions we conclude that, (1) source distribution plays a critical role in determining the modelled patterns of scalar concentrations and fluxes over hills covered by tall canopies, and (2) the scalar fields modelled here over an isolated ridge are qualitatively similar to those seen in previous studies with periodic ridges. The scalar fields are dominated by flow-related changes in the turbulent mixing and the flow separation within the canopy over the lee slope. Earlier conclusions around scalar transport in complex terrain (e.g. around scaling arguments) are thus more widely applicable to a range of hill geometries.

The topographic impacts on scalar concentrations and vertical fluxes are strongly dependent on the distribution and type of sources contributing to the scalar. The relative impact is larger for scalars with sources near the ground since the topography has a relatively larger impact on the flow and turbulence field near the ground. The net topographic impact on scalars with multiple sources (e.g. net canopy CO_2 assimilation and ground respiration) is sensitive to the balance in distribution and strength of the sources, so assessing possible errors using simple rules-of-thumb is not practical. For scalars whose sources are determined though concentration boundary conditions (and by inference mixed boundary conditions, e.g., temperature or water vapour), correlations in space between the flow perturbations and the scalar concentrations lead to spatial variations in the source strength that can be sufficient to lead to a landscape-averaged source strength that differs from the background, no-terrain, case.

The topographic impacts simulated are seen even for very gentle topography (slopes of $\approx 2.5°$ are considered) and can occur well away from topography (discernible impacts occur up to $2.5L$ away from ridge crest) and in neutrally stratified flow. The inherent smoothing that occurs with long-time averaging, including over wind direction, will tend to reduce the potential for biases in eddy-covariance estimates of scalar exchange over complex terrain but cannot guarantee to remove all such biases. We have considered purely the impacts of topography on short time-period concentrations and fluxes. The variability and sensitivity in the impacts will be manifest as variability in the longer-term relationships between scalar exchanges and their climatological drivers. We conclude that eddy-covariance data require interpretation within the topographic context at all sites.

References

Aubinet M, Berbigier P, Bernhofer CH, Cescatti A, Feigenwinter C, Granier A, Grünwald TH, Havrankova K, Heinesch B, Longdoz B, Marcolla B, Montagnani M, Sedlak P (2005) Comparing CO2 storage and

advection conditions at night at different CARBOEUROFLUX sites. Boundary-Layer Meteorol 116:63–94. doi:10.1007/s10546-004-8

Belcher SE, Newley TMJ, Hunt JCR (1993) The drag on an undulating surface induced by the flow of a turbulent boundary layer. J Fluid Mech 249:557–596. doi:10.1017/S0022112093001296

Belcher SE, Finnigan JJ, Harman IN (2008) Flows through forest canopies in complex terrain. Ecol Appl 18:1436–1453. doi:10.1890/06-1894.1

Belcher SE, Harman IN, Finnigan JJ (2012) The wind in the willows: flows in forest canopies in complex terrain. Annu Rev Fluid Mech 44:479–504. doi:10.1146/annurev-fluid-120710-101036

Bohrer G, Katul GG, Walko RL, Avissar R (2009) Exploring the effects of microscale structural heterogeneity of forest canopies using large-eddy simulations. Boundary-Layer Meteorol 132(3):351–382. doi:10.1007/s10546-009-9404-4

Feigenwinter C, Bernhofer C, Eichelmann U, Heinesch B, Hertel M, Janous D, Kolle O, Lagergren F, Lindroth A, Minerbi S, Moderow U, Mölder M, Montagnani L, Queck R, Rebmann C, Vestin P, Yernaux M, Zeri M, Ziegler W, Aubinet M (2008) Comparison of horizontal and vertical advective CO$_2$ fluxes at three forest sites. Agric For Meteorol 148(1):12–24. doi:10.1016/j.agrformet.2007.08.013

Finnigan JJ (1999) A comment on the paper by Lee (1998) On micrometeorological observations of surface-air exchange over tall vegetation. Agric For Meteorol 97:55–64. doi:10.1016/S0168-1923(99)00049-0

Finnigan JJ (2000) Turbulence in plant canopies. Annu Rev Fluid Mech 32:519–571. doi:10.1146/annurev.fluid.32.1.519

Finnigan JJ (2004) The footprint concept in complex terrain. Agric For Meteorol 127:117–129. doi:10.1016/j.agrformet.2004.07.008

Finnigan JJ, Belcher SE (2004) Flow over a hill covered with a plant canopy. Q J R Meteorol Soc 130:1–29. doi:10.1256/qj.02.177

Finnigan JJ, Harman IN, Ross AN, Belcher SE (2015) First order turbulence closure for modelling complex canopy flows. Q J R Meteorol Soc (in press)

Goulden ML, Miller SD, da Rocha HR (2006) Nocturnal cold air drainage and pooling in a tropical forest. J Geophys Res Atmos 111(D8):D08S04. doi:10.1029/2005JD006037

Grant ER, Ross AN, Gardiner BA, Mobbs SD (2015) Field observations of canopy flow over complex terrain. Boundary-Layer Meteorol Online First:1–21, doi:10.1007/s10546-015-0015-y

Harman IN, Finnigan JJ (2008) Scalar concentration profiles in the canopy and roughness sublayer. Boundary-Layer Meteorol 129(3):323–351. doi:10.1007/s10546-008-9328-4

Harman IN, Finnigan JJ (2010) Flow over hills covered by a plant canopy: extension to generalised two-dimensional topography. Boundary-Layer Meteorol 135(1):51–65. doi:10.1007/s10546-009-9458-3

Harman IN, Finnigan JJ (2013) Flow over a narrow ridge covered with a plant canopy: a comparison between wind-tunnel observations and linear theory. Boundary-Layer Meteorol 147(1):1–20. doi:10.1007/s10546-012-9779-5

Huang J, Katul G, Albertson J (2013) The role of coherent turbulent structures in explaining scalar dissimilarity within the canopy sublayer. Environ Fluid Mech 13:571–599. doi:10.1007/s10652-013-9280-9

Hunt JCR, Leibovich S, Richards KJ (1988) Turbulent shear flow over low hills. Q J R Meteorol Soc 114:1435–1470. doi:10.1002/qj.49711448405

Katul GG, Poggi D (2010) The influence of hilly terrain on aerosol-sized particle deposition into forested canopies. Boundary-Layer Meteorol 135:67–88. doi:10.1007/s10546-009-9459-2

Katul GG, Poggi D (2011) A note on aerosol sized particle deposition onto dense and tall canopies situated on gentle cosine hills. Tellus B 63:395–400. doi:10.1111/j.1600-0889.2011.00528.x

Katul GG, Poggi D (2012) The effects of gentle topographic variation on dispersal kernels of inertial particles. Geophys Res Lett 39:L03401. doi:10.1029/2011GL050811

Katul GG, Finnigan JJ, Poggi D, Leuning R, Belcher SE (2006) The influence of hilly terrain on canopy-atmosphere carbon dioxide exchange. Boundary-Layer Meteorol 118:189–216. doi:10.1007/s10546-005-6436-2

Leuning R, Zegelin SJ, Jones K, Keith H, Hughes D (2008) Measurement of horizontal and vertical advection of CO$_2$ within a forest canopy. Agric For Meteorol 148:1777–1797. doi:10.1016/j.agrformet.2008.06.006

Patton EG, Katul GG (2009) Turbulent pressure and velocity perturbations induced by gentle hills covered with sparse and dense canopies. Boundary-Layer Meteorol 133:189–217. doi:10.1007/s10546-009-9427-x

Poggi D, Katul GG (2007) Turbulent flows on forested hilly terrain: the recirculation region. Q J R Meteorol Soc 133:1027–1039. doi:10.1002/qj.73

Raupach MR, Weng WS, Carruthers DJ, Hunt JCR (1992) Temperature and humidity field and fluxes over low hills. Q J R Meteorol Soc 118:191–225. doi:10.1002/qj.49711850403

Raupach MR, Finnigan JJ, Brunet Y (1996) Coherent eddies and turbulence in vegetation canopies: the mixing length analogy. Boundary-Layer Meteorol 78:351–382. doi:10.1007/978-94-017-0944-6-15

Ross AN, Vosper SB (2005) Neutral turbulent flow over forested hills. Q J R Meteorol Soc 131:1841–1862. doi:10.1256/qj.04.129

Ross AN (2008) Large eddy simulations of flow over forested ridges. Boundary-Layer Meteorol 128:59–76. doi:10.1007/s10546-008-9278-x

Ross AN (2011) Scalar transport over forested hills. Boundary-Layer Meteorol 141:179–199. doi:10.1007/s10546-011-9628-y

Tracktenbrot A, Katul GG, Nathan R (2014) Mechanistic modeling of seed dispersal by wind over hilly terrain. Ecol Model 274:29–40. doi:10.1016/j.ecolmodel.2013.11.029

van Gorsel E, Leuning R, Cleugh HA, Keith H, Suni T (2007) Nocturnal carbon efflux: Reconciliation of eddy covariance and chamber measurements using an alternative to the u(*)-threshold filtering technique. Tellus B 59(3):397–403. doi:10.1111/j.1600-0889.2007.00252.x

van Gorsel E, Leuning R, Cleugh HA, Keith H, Kirschbaum MUF, Suni T (2008) Application of an alternative method to derive reliable estimates of nighttime respiration from eddy covariance measurements in moderately complex topography. Agric For Meteorol 148(6–7):1174–1180. doi:10.1016/j.agrformet.2008.01.015

Zeri M, Rebmann C, Feigenwinter C, Sedlak P (2010) Analysis of short periods with strong and coherent CO_2 advection over a forested hill. Agric For Meteorol 150(5):674–683. doi:10.1016/j.agrformet.2009.12.003